NGU
Norges geologiske undersøkelse
Geological Survey of Norway

Offprint NGU Bulletin 409, 49—72

MICHAEL HEIM, TOR GRENNE & TORE PRESTVIK

The Resfjell Ophiolite Fragment, Southwest Trondheim Region, Central Norwegian Caledonides

Trondheim 1986

The Resfjell Ophiolite Fragment, Southwest Trondheim Region, Central Norwegian Caledonides

MICHAEL HEIM, TOR GRENNE & TORE PRESTVIK

Heim, M., Grenne, T. & Prestvik, T. 1987: The Resfjell ophiolite fragment, southwest Trondheim region, central Norwegian Caledonides. *Nor. geol. unders. Bull 409*, 49-71.

The Resfjell complex of Meldal, southwestern Trondheim region, provides an almost ideal cross-section through the uppermost part of an ophiolite. The stratigraphically lowest rocks exposed are metagabbro and microgabbro wich are followed by a sheeted dyke complex, a transition zone composed of hyaloclastites, pillow lavas and 10-30% dykes. These are succeeded by two lava units, lower and upper, which are separated by a sequence of volcaniclastic sediments in the eastern part of the area. The assemblage of ophiolitic rocks is exposed over a c. 5 km N–S section. The entire complex is inverted with moderate to steep dips, and has tectonic contacts towards both the south and the north. Subordinate, non-economic sulphide mineralizations occur in zones parallel to dykes in all units below the upper pillow lavas. Geochemical data show that the dykes and lavas are tholeiitic and of typical ocean floor or extensional basin type basalt. The upper pillow lavas, however, are somewhat more evolved. This is interpreted as due to extensive fractional crystallization. Based on information from neighbouring ophiolite fragments, where subduction-relatead volcanic rocks are interbedded with tholeiitic metabasalts correlated with the Løkken ophiolite fragment, it is considered that the ocean floor type of metabasalts of Resfjell and nearby Grefstadfjell represent magmatism of a very early extensional stage above newly subducted oceanic crust, or alternatively in a very wide marginal basin. It is tentatively suggested that these basalts were formed before the underlying mantle wedge became enriched in mobile LIL elements from the subducted oceanic lithosphere.

M. Heim, T. Grenne & T. Prestvik, Geologisk Institutt, N-7034 Trondheim-NTH, Norway.

Introduction

In recent years the allochthonous Lower Paleozoic metavolcanic and metasedimentary rock sequences of the western Trondheim region have been intensively investigated, and general syntheses of the district have been presented by Roberts (1978), Oftedal (1980, 1981), Roberts & Wolff 1981) and Roberts et al. (1984). Metabasaltic greenstone units are one of the main magmatic components in this part of the Caledonian allochthon (Grenne 1979, Grenne et al. 1980, Grenne & Roberts 1981, 1983). Tectonically the region is characterized by complicated imbrication and fold structures, making correlations along and across the main Caldeonian strike direction difficult, even over short distances.

The ophiolite-hosted massive stratiform Fe-Cu-Zn sulphide deposits at Løkken have made the region attractive also from the economic point of view. It was this aspect that led to the field investigations in the Resfjell area by one of the authors (M.H.) in the summer of 1983; the preliminary results of this study have been described by Heim (1984).

Geological setting

The mountain Resfjell is situated to the west of the Orkdal valley in the Meldal district, 60 km southwest of Trondheim (Fig. 1). According to the latest geological maps (Wolff 1976, Guezou 1981) it lies within, but close to the south-southwestern border of the so-called 'Støren Nappe' (Gale & Roberts 1974), the highest tectonic unit within the western part of the Trondheim Nappe Complex. This complex belongs to the Upper Allochthon in this segment of the Scandinavian Caledonides (Gee et al. 1985). A regional stratigraphy of part of the area was established by Vogt (1945). This has later been modified by Gale & Roberts (1974), Wolff (1979), Oftedahl (1980), Ryan et al. (1980), and Oftedahl & Prestvik (1985). Distribution of the main sequences within the 'Støren Nappe' is shown in Fig. 1.

The relationship between the various greenstone complexes of the western Trondheim district is somewhat ambiguous, as discussed by Grenne (1986), although they have previously all been correlated to the Støren Group in the southeast (Vogt 1945). The Støren Group of the

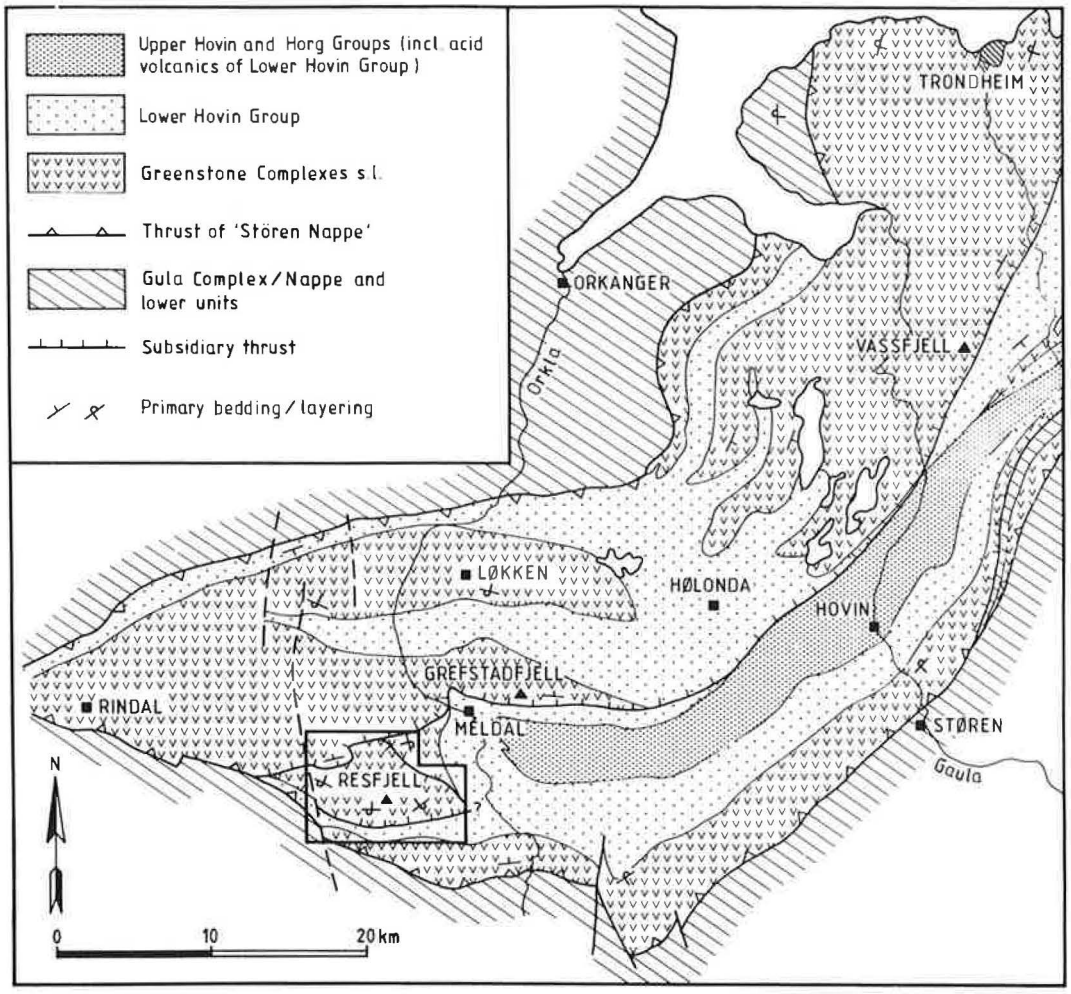

Fig. 1. Sketch map of the southwestern Trondheim region indicating major lithological and structural features and the location of the Resfjell ophiolite fragment.

type area is thought to have been obducted on to the Gula Complex and initially deformed during the Finnmarkian event in earliest Ordovician times, prior to deposition of the overlying Lower and Upper Hovin and Horg Groups (Furnes et al. 1980). The commonly used term 'Støren Nappe' for the Støren, Lower and Upper Hovin and Horg Groups *together* (introduced by Gale & Roberts 1974) is misleading, as stressed by Grenne (1986). Furthermore, Ryan et al. (1980) suggested that the ophiolite complex of Grefstadfjell, immediately north-northeast of the Resfjell area, actually occurs within the Lower Hovin Group and was related to a short-lived, late Arenig, spreading event. The proposed maximum age of mid-Arenig was based mainly on the relations between a few metres thick unit of tuffs and breccias in the Lo valley and fossiliferous metasediments of the underlying Lo Formation and overlying Bogo shales. However, the correlation between this volcanic unit and the main Grefstadfjell greenstone is at best dubious as similar thin greenstone units occur within the Lower Hovin Group elsewhere in the area. These are clearly separate from and younger than the thick greenstone complexes (Chaloupsky 1970).

Despite the possibility that the Støren Group *s.s.* could be of pre-Finnmarkian age while the other western Trondheim district ophiolites

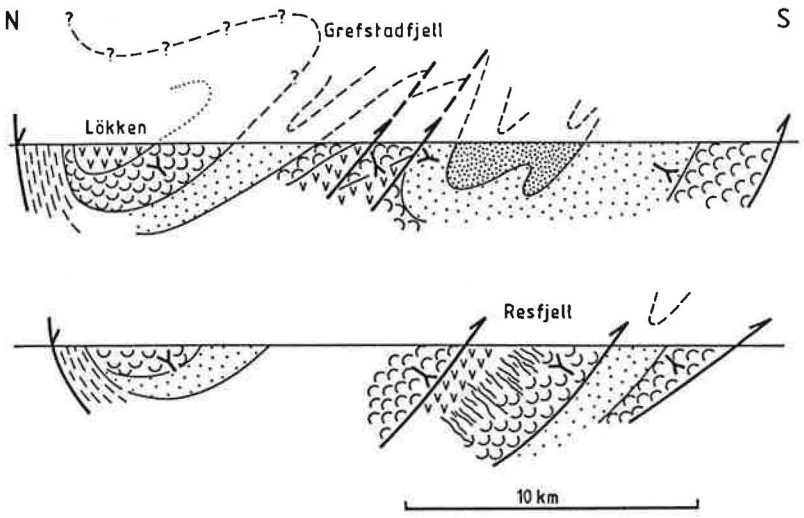

Fig. 2. Simplified schematic N-S cross-section through ophiolite fragments of the western Trondheim region.

could be younger (Roberts et al. 1984), all these thick metabasaltic sequences show many similarities. Apart from the igneous rocks, they include extensive horizons of jasper and characteristic mixed sulphide-oxide-silicate iron-formations (Grenne et al. 1980, Sand 1986), as well as abundant Fe-Cu-Zn sulphide mineralizations both of massive stratiform type within the lava pile (Grenne et al. 1980, Grenne 1986) and of cross-cutting veins of disseminated type in various parts of the grabbro—sheeted dykes—lava section (Kjeldsen 1984, Grenne 1986). The similarities in associated lithologies may be taken to imply that the separate sequences are correlatable (perhaps with the exception of the Støren Group *s.s.*). In particular, this is true when comparing the Vassfjell and Løkken ophiolites (Grenne et al. 1980). Vassfjell and Grefstadfjell were interpreted by Roberts et al. (1984) as occupying the normal limb, and Løkken the inverted limb, of a major SE-facing F1 isoclinal fold-nappe. The Resfjell complex is lithologically and petrochemically nearly identical to the Grefstadfjell ophiolite (see below). The former is in an inverted position, but both have tectonic contacts to the Caradocian Kalstad limestone (which they overlie structurally) to the south (cf. map, Plate 1 and Chaloupsky 1977). Thus, it is possible that the Resfjell complex is part of the inverted limb of another synclinal fold-nappe to the south. The contact between the two fold-nappes is tentatively correlated with a subsidiary fault (Figs. 1 & 2). The fact that the tectonic contact with the Kalstad limestone is bent around and partly follows this large fold structure (Plate 1), while it apparently has truncated the next, right-way-up limb of the recumbent fold structure, suggests that movements along this tectonic contact were more or less contemporaneous with the formation of the recumbent fold-nappe.

The Resfjell and the Grefstadfjell ophiolite fragments show great similarities with respect to both lithology and geochemistry of the igneous rocks. For this reason, hitherto unpublished chemical data from Grefstadfjell are included in the discussion of the igneous geochemistry. The Grefstadfjell unit comprises gabbros at its present base which pass upwards into a 100% sheeted dolerite-dyke complex, and then into 1.1 km of pillow lavas (Ryan et al. 1980, Roberts et al. 1984). The upper, approximately 350 m of the lava pile interdigitates with sediments which, according to Ryan et al. (1980), belong to the Lower Hovin Group. A graptolite fauna suggests an uppermost Arenig age for these sediments.

The Resfjell ophiolite fragment (Plate 1) has an E-W extended triangular shape, covering an area of about 30 km². The rock suite widens and youngs towards the south and shows moderate to steep inverted northward dips. Deformation is comparatively weak, especially in eastern and central areas (Goråsfjellet—Resfjell, Plate 1). A NW-SE trending schistosity increases in intensity towards the west and southwest (Småfjella—Snipvatna, Plate 1), and all the rocks show low-grade metamorphic mineral parageneses. Contacts with the surrounding units have the

character of steeply dipping (thrust-) faults with variable degrees of cataclasis. The neighbouring rocks are greenstones to the northwest and northeast, and mainly Hovin-type metasediments to the southwest and south.

The Resfjell ophiolite pseudostratigraphy

The Resfjell ophiolite pseudostratigrahpy is shown in Fig. 3. A description of the individual members of the sequence is given below.

Leucogabbro

This rock-type is a strongly altered leucogabbro (mafic colour index M=15-45) with up to 1.5 cm long, often poikilitic, amphibole crystals and white saussurite after hypidiomorphic plagioclase. Two types of amphibole are present: i) a homogeneous, pale green variety, in some cases with brownish cores, probably of late magmatic origin, and ii) fibrous aggregates partly altered to chlorite. The latter are interpreted as altered from pyroxene. In the southeast some leucocratic anorthositic metagabbros are present. These may be feldspar cumulates. Near the contacts to surrounding rocks the gabbros have a more porphyritic appearance with an outwards decreasing proportion of plagioclase phenocrysts in a dark, fine-grained matrix. Southwest of point 914 (Plate 1), and in the far southeast, the leucogabbro clearly intrudes pillow lavas. On the other hand, there are several places where the gabbros are intruded by dolerite dykes. The field evidence suggests that gabbroic magma, in a partly crystallized form, intruded the sheeted dyke — pillow lava transition zone. The gabbro was later intruded by dykes that were probably feeders to stratigraphically higher pillow lavas.

Microgabbro

This is an almost completely altered dark gabbro (M=50) with an originally granular, fine-grained (0.4mm) texture. It consists of saussurite (clinozoisite/epidote + albite), after primary basic plagioclase, actinolite, chlorite, leucoxene after Fe-Ti oxides, and relict apatite.

About 1 km northwest of Midtfjellet (Plate 1) the rock has a quite homogeneous appearance and no mineral layering is observed. There is, however, apparently a gradual transition into the dyke complex towards the south where chilled margins are observed locally. Several inclusions of leucogabbro (up to 100 m) are found. West of point 779 (Plate 1) microgabbro dykes or veins transect the leucogabbro in a braided pattern. A general lack of clear, fine-grained chilled margins in the microgabbro suggests that it was intruded immediately after the leucogabbro, perhaps while the latter was still hot.

Sheeted dyke complex

In an up to 1.2 km wide zone east and west of Midtfjellet (Plate 1), subvertical (generally steeply NE-dipping) doleritic dykes form a well developed sheeted dyke complex virtually with 100% dykes. Dyke thickness varies from a few cm to 5 m although it is generally in the range 0.5—1.5 m, which is common for ophiolite dyke complexes (Rosencrantz 1983). There is an increase in preservation of chilled margins and good ophitic textures from north to south. Generally the dykes are subparallel, but acute intersection angles as well as dyke-in-dyke and one-way-chilled relations are quite common. Most dykes are subophitic fine- to medium-grained metadolerites.

Apart from relict augite observed in one thin-section, the dyke rocks are completely altered, in part pseudomorphically. Mafic silicates are replaced by actinolitic hornblende, fibroblastic actinolite and chlorite. Plagioclase is saussuritized and primary oxides are transformed to leucoxene. Subordinate porphyritic dykes with up to 35% plagioclase phenocrysts are probably related to the leucogabbros.

Transition zone

The transition from 100% dykes (Fig. 4) to well pillowed basaltic lavas occurs in a zone varying from 0.3—1.2 km in width. Besides the gradual substitution of dykes by pillow lavas, this zone is characterized by widespread brecciation and a high percentage of hyaloclastite material with distinct orange-brown surface colour and a knotty weathered surface.

The lavas are light-coloured, irregularly pillowed, basaltic greenstones with dark rims and much 'matrix' between the pillows. This matrix is rich in yellow-green epidote and dark hyaloclastite fragments. The pillows are usually small and have fingers and buds, features characteristic for 'knobbly pillow lavas' (Ballard & Moore 1977) and probably indicative of relatively high eruptive flow rates (causing high liquid pressure in the pillows and subsequent rupturing of the thin pillow crusts with formation of numerous new 'daughter' pillows). Locally, concordant

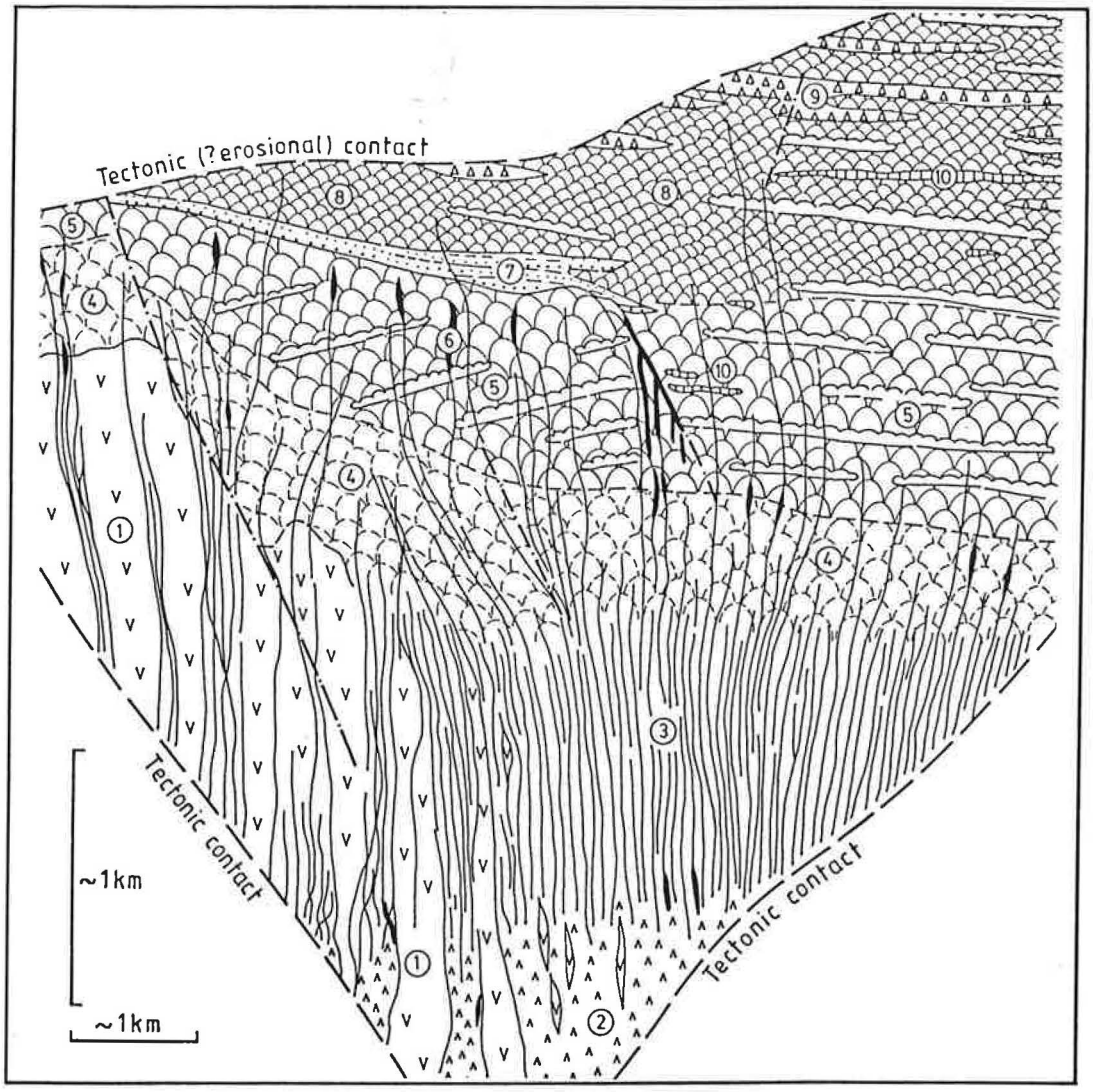

Fig. 3. Interpreted cross section and pseudostratigraphy of the Resfjell ophiolite fragment.

Tectonic contact to Hovin Group sediments.

Upper pillow lava (8):
Basaltic lavas with diffuse broad rims to pillows, commonly variolitic. Pillow breccias (9) and jasper horizons (10). Preserved thickness up to 1000 m.

Volcaniclastic sediments (7):
Fining upward sequences; party interfingering with upper pillow lavas. Total thickness up to 200 m.

Lower pillow lava(5):
Close-packed, large-pillowed basaltic lavas with thin rims; subordinate massive flows. Drained hollow and shelved pillows common. Sulphide mineralizations (6) are usually associated with dykes. Approximate thickness 800 m.

Transition zone (4):
Irregularly pillowed/brecciated basaltic lavas and dykes rich in hyaloclastic material; upward decreasing dyke density. Approxte thickness 300—1500 m.

Sheeted dyke complex (3):
Up 100% metadolerite dykes. Total thickness < 1000 m.

Microgabbro (2):
Fine-grained, dark gabbro.

Leucogabbro (1):
Coarse-grained, altered leucogabbro (plagioclase cumulate gabbro?).
Tectonic contact at base.

Fig. 4. Multiple dykes intruding a hyaloclast-rich pillow lava (upper right) in the transition zone, close to the top of Resfjell.

layers of hyaloclastic breccia up to several metres thick are observed. The fragments in these represent pillow-fingers, 'glassy' rims and fine-grained greenstone and are set in a matrix of sandy lava detritus.

Another characteristic feature is zones of 'in situ' brecciation of both dykes and lavas. The rocks were apparently broken up during or shortly after solidification. This resulted in fragmentation where the single pieces were slightly rotated. The breccia zones are commonly parallel to dykes, and show increasing brecciation towards dyke contacts. They probably represent fault zones which were intruded by dykes under a tensional stress regime as described by Rosencrantz (1983). In other places, chilling of hot rock by percolating seawater may have caused brecciation and fragmentation.

Between Resfjell and Goråsfjellet (Plate 1), fine-grained, homogeneous lavas of possible sheet-flow type (Ballard et al. 1979) dominate. These are also thought to reflect high rates of lava delivery.

Mineralogically the lavas of this zone are fibroblastic, fine-grained (<0.2 mm) chlorite-leucoxene-bearing albite-epidote-actinolite felses with relict plagioclase phenocrysts (<2 mm). Pillow rims consist of fibrous parallel-oriented green chlorite. Hypidioblastic (<1 mm) epidote dominates the matrix between pillows and shows helicitic growth, starting from rims and fissures of 'glass' fragments. Concentric zonation in 'glass' fragments is represented by chains of idioblastic sphene crystals.

Lower pillow lava

In an up to 1 km wide zone close-packed, light-coloured, pillow lavas with thin (1 cm), distinct, dark 'glassy' rims predominate (fig. 5). Their various characteristic features are: (1) Varying size of pillows, although large pillows (0.5-1.0 m across) predominate. (2) Apparently equidimensional pillows of 'bulbous' type are abundant; partly branched, elongate pillows occur locally. The apparent predominance of 'bulbous' pillows may not be a real feature in view of the general lack of three-dimensional exposures. (3) Flat pillows ('mattress' type). These are interpreted as bulbous pillows that were flattened due to drainage of lava while the pillows were still plastic. (4) Hollow layered pillows with (up to 32) internal, subparallel lava shelves are common (Fig. 6). These are the product of stepwise drainage during solidification (cf. Ballard & Moore 1977, Grenne & Roberts 1983). Cavities between shelves are now partly filled with secondary calcite, epidote and quartz. (5) Collapsed pillows with overlying thin hyaloclastic breccia. These may represent tops of pillow lava flows.

In the lower pillow lavas massive lava flows

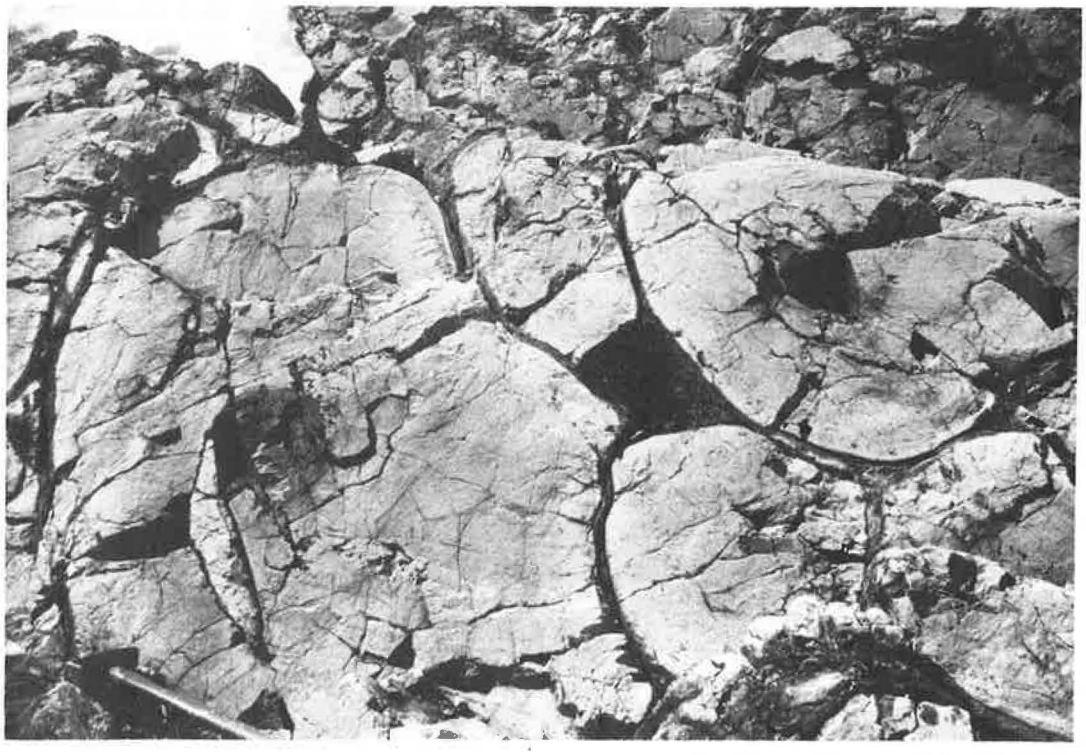

Fig. 5. Closely packed pillows with thin, dark selvages of altered glass. Lower pillow lava, south-eastern flank of Resfjell.

(<15 m thick) are abundant. Locally these flows have preserved columnar, polygonal jointing (Fig. 7).

The metamorphic mineralogy of lavas from this zone includes: fibroblastic actinolite (15-55%), chlorite (7-25%), granular clinozoisite (5-25%), sphene/leucoxene (4-10%), albite (15-60%) and calcite (≦2%). In the massive lava flows ophitic textures are abundant. Other relict textures are: i) plagioclase phenocrysts (≦4 mm), commonly reflecting flow patterns in the lavas, and ii) small vesicles (≦0.7 mm) filled with secondary epidote, chlorite and calcite.

Volcaniclastic sediments

In the eastern part of the map area (Plate 1) the lower pillow lavas are overlain by a sequence of predominantly coarse clastic metasediments. The greatest thickness (c. 200 m) is found just east of the branched, western termination of the zone, where the sediments interfinger with upper pillow lavas. In the east, near Blautsetra, the zone is about 30 m wide and the sediments are here truncated along the plane of discontinuity towards the Hovin-type sediments.

The sediments represent an immature, coarse clastic unit with fining upwards (now inverted) sequences. The main part consists of polymict matrix- to clast-supported breccias and minor conglomerates. Major clast components are fine-grained basaltic greenstone, gabbro, jasper, milky quartz and bluish-red slate. More exotic fragments, such as felsic rocks of possible volcanic origin, albite-porphyrite and trondhjemite, occur as minor constituents.

Fine-grained conglomeratic as well as sandy and silty layers usually show distinct (often cyclic) grading and other primary features such as foreset bedding, downcutting channels, rip-up clasts of silty material in sandy layers, and flame structures. The more silty beds are generally bluish-red (coloured by hematite), whereas the sandstones are grey to green. Concentrations of heavy minerals such as magnetite, zircon and tourmaline have been observed in a few places.

It is suggested that this sequence of volcaniclastic sediments is largely the product of periodic submarine slides. The overall tendency towards fining upward suggests a decreasing relief.

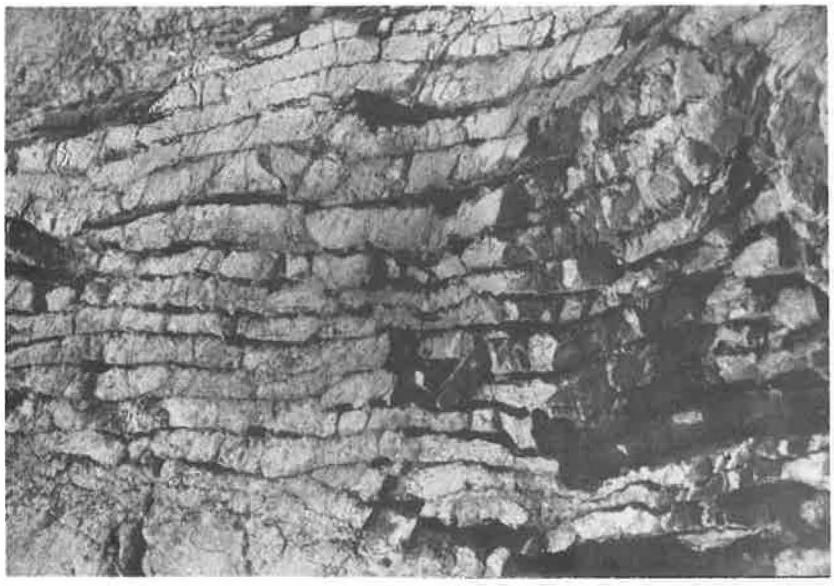

Fig. 6. Subparallel shelves from the interior of a drained pillow from the lower pillow lava. South-eastern flank of Resfjell.

Upper pillow lava

The upper pillow lavas are generally darker green than the lower ones. The pillows show broad, chlorite-rich, dark-green rims with a diffuse transition towards the pillow interior. Variolitic textures are common, especially in pillow rims. Varioles and pillow cores are usually rich in yellow-green epidote. Pillow lavas rich in stilpnomelane occur locally, and reflect a high content of iron and a high Fe/Mg ratio.

Small pillows ($\leqq$0.5 m) with epidote-rich matrix predominate. Furthermore, elongate pillows, with the longest pillow axis plunging slightly towards west-northwest, are also common.

Within the upper pillow lava zone there are some massive, concordant dolerites up to 50 m thick. In their central parts these dolerites are coarse-grained with up to 7 mm long hypidiomorphic hornblende crystals. Vesicles are filled with aggregates of chlorite and epidote. These units are interpreted as thick massive lava flows. Apart from stilpnomelane in some of the lavas, the mineralogy is the same in this zone as in the lower pillow lavas.

In the western, uppermost part of the upper pillow lavas, breccia layers of varying type and extent are quite common. The dominating type comprises angular fragments of pillows, in part with preserved rims, and locally whole pillows. The matrix consists of finer lava debris and commonly has a porous appearance.

In the same area several red to greyish-coloured beds of jasper (up to 4 m thick) are found, mostly in the uppermost part of the zone. One main level can be followed from east-southeast of Snipvatna (Plate 1) for more than 3 km northwestwards to lake 690. There, fine-grained, thin-banded magnetite/stilpnomelane-rich sediments (with albite predominating over quartz) occur together with the jasper bed, and resemble to some extent the banded iron-formations in the Løkken area (Sand 1986).

In the eastern part of the area the upper pillow lavas and their assosiated rocks (massive lava flows, pillow breccias, jaspers and associated rocks) are separated from the lower volcanites by the volcaniclastic sediments, with which they partly interfinger. They were probably formed in an environment with a considerable topographic relief. This is indicated by the abundant lava breccias, which may be interpreted as talus deposits. It is not clear whether volcanic activity in the southwest was continuous from the lower to the upper pillow lava series. The fact that the intercalated volcaniclastic sediments contain much jasper debris may indicate that volcanic activity in the west was contemporaneous with sedimentation in the east. The association of jasper beds with the upper pillow lava accords with that found in the Løkken area (Grenne et al. 1980).

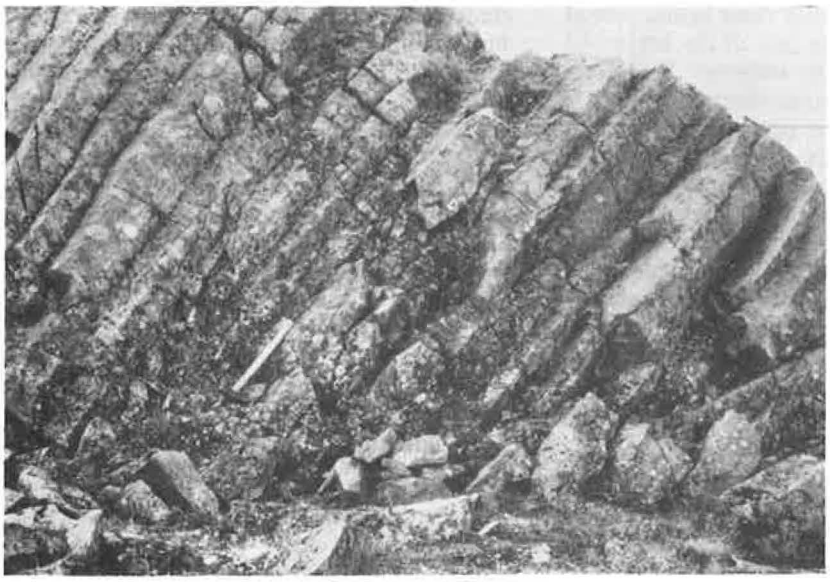

Fig. 7. Polygonal columnar jointing of lava flow, southern flank of Resfjell.

Dolerite dykes and dyke swarms in the lava units

Cross-cutting dykes and dyke swarms with obvious chilled margins are numerous in all types of lavas. Petrographically they cannot be distinguished from the dolerites in the upper part of the sheeted dyke complex. Although direct transitions from dyke to lava have not been observed in the field, the general decrease in dyke density upwards tends to suggest that the dykes represent feeders to the lavas. The lack of recognisable dykes in the Snipvatna area (Plate 1) can be the result of tectonic deformation. Here, flattening and inhomogeneous shear may have obliterated primary cross-cutting relations.

Sulphide mineralizations

Small concentrations of sulphides are found in various parts of the ophiolite sequence, from the microgabbros up to near the lower/upper pillow lava boundary. These are all in the form of disseminations or cross-cutting veins; no stratiform sulphide deposits are known in the Resfjell complex although this type is abundant in the Løkken area to the north (Grenne et al. 1980) and is also found in the Grefstadfjell ophiolite fragment. The sulphide occurrences comprise pyrrhotite, chalcopyrite, pyrite and locally subordinate sphalerite together with some quartz in 1-10 cm thick veins. Most of these zones are parallel or subparallel to the general dyke trend, and many are either located close to the actual dyke contacts or form disseminations within and along dykes. Some mineralized zones can be traced more or less continuously across a stratigraphic interval of nearly 1 km within the lower pillow lavas. (Plate 1). Associated with the mineralizations there is a variable alteration of the host rocks, giving chlorite (± stilpnomelane)-albite-quartz assemblages or, by more pervasive alteration, chlorite-stilpnomelane-quartz (Kjeldsen 1984). Epidote-actinolite-chlorite alteration assemblages with greatly modified chemistry (cf. Table 1, sample R10) are found locally. The most common chemical effects of the alteration are loss of calcium (cf. Table 1, samples R16 and R17) and in some cases sodium in the chlorite-quartz rocks, accompanied by a marked increase in silicate-bound iron and manganese.

Both alteration assemblages and mineralizations are comparable to those found in the hydrothermal feeder-zones to massive stratiform sulphide deposits in the Løkken area (Grenne 1986), except for the general predominance of pyrite over pyrrhotite in the latter. The similarities suggest that the Resfjell mineralizations also formed from ascending hydrothermal solutions within the original oceanic crust (e.g. Mottl 1983), although here there is no direct evidence that the metal-bearing solutions reached the sea-floor and precipitated massive sulphides.

Thus, it is difficult to relate these hydrothermal processes to any specific part of the magmatic evolution of the ophiolite sequence. It is noteworthy, however, that mineralizations are generally lacking in the upper pillow lavas, whereas in the lower pillow lavas, especially in the central and eastern areas, sulphide occurrences are particularly abundant between 100 and 300 m stratigraphically below the sedimentary unit. This places the main hydrothermal mineralization 'event' close to the boundary between the lower and upper pillow lavas, which is comparable to the situation at Løkken (Grenne et al. 1980, Grenne 1986).

Hovin-type metasediments

In the southern part of the map area a sequence of Hovin-type sediments is present. The contact between these rocks and the Resfjell ophiolite complex is tectonic and discordant with respect to both rock suites. These metasediments, which include polymict conglomerates, greenish metasandstones and phyllites, fine-grained, blue-grey marble (in part biosparitic) and felsic metavolcanites, will not be described in detail here.

Geochemistry

Sampling and analytical procedure

Major element analyses of 35 samples are used in this study. Ten of these are taken from Holub (unpubl. NGU data) and 8 from Kjeldsen (1984). Fifteen greenstone samples from the adjacent Grefstadfjell ophiolite are included for comparison. All the samples are analysed by X-ray fluorescence (XRF) at NGU or Geol. Inst., NTH, on fused glass beads according to standard methods. International standards with the recommended values of Flanagan (1973) were used. Na_2O was determined by flame photometry at NGU or atomic absorbtion spectrometry at NTH (see Tables 1 & 2 for specifications). Twenty-eight of the samples were analysed for Zr, Y, Sr, Rb, Ba, Zn, Cu, Ni, Cr, V at NGU or NTH by XRF on pressed powder pellets with international standards and recommended values of Flanagan (1973) for calibration. Thirteen samples from Resfjellet were selected for analysis of the rare earth elements La, Ce, Nd, Sm, Eu, Tb, Yb and Lu as well as Sc, Hf, Ta and Th. Ce and Nd were analysed on mass spectrometer, the other elements by instrumental neutron activation at IFE, Kjeller, using BCR-1 for calibration and GSP-1 for control.

The analyses taken from Kjeldsen (1984) are on samples which were collected adjacent to sulphide mineralizations (samples no. R15, R16, R17), and samples no. R9 and R10 are doleritic greenstones within mineralized zones. These rocks may obviously be more or less affected by alteration and are thus excluded from diagrams involving the 'mobile' elements Fe and Mg. The other samples are thought to be representative of the various parts of the sequence. These are fresh and unweathered. Samples of strongly sheared or veined greenstones, as well as chilled margins of dykes or pillows, have been avoided.

Results

The major and trace element analyses of upper and lower lava members, dykes and gabbros from the Resfjell area are shown in Table 1. Analyses from the Grefstadfjell complex (Table 2) are from the main central part of the ophiolite fragment, except for samples NG1, NG2 and NG3 which are from the northernmost part, where the metabasalts interdigitate with breccias and sedimentary units (Ryan et al. 1980). One of the Resfjell dyke samples (R11) is distinctly different from the other dykes and lavas and is much more akin to the north Grefstadfjell metabasalts. This dyke sample is, therefore, treated separately in the diagrams and following discussion.

All analysed dykes and lavas in the Resfjell and Grefstadfjell area are basaltic, with SiO_2 values ranging from 45% to 50.6%, and 46.3% to 51.6%, respectively (excluding the mineralized samples). K_2O is uniformly very low (less than 0.01% up to 0.27%) in the main greenstone complexes, and although K_2O, Na_2O and SiO_2 are known to be susceptible to changes during submarine alteration processes and metamorphism (Pearce 1976), a SiO_2-alkali plot (not shown) displays a fairly dense clustering well below the alkaline/subalkaline division line of Irvine & Baragar (1971). The northern Grefstadfjell (NG) metabasalts and dyke R11, however, have significantly higher total alkalis, K_2O and Ba at similar SiO_2 contents, indicating that these rocks may be transitional towards an alkaline magma type. It must be emphasized, however, that all these elements may have suffered considerable changes in concentration due to secondary processes (Pearce 1976).

Plots of TiO_2 and FeO(tot.) vs. FeO(tot.)/MgO ratio (Fig. 8) show that the majority of samples define trends of strong TiO_2 and iron enrichment, very close to the typical differentiation trends of abyssal tholeiites (Miyashiro 1975). In Fig. 8 the NG metabasalts and dyke R11 demonstrate their distinctive transitional chemistry, plotting between the trends of abyssal tholeiites and the alkaline Kilauean series. Both sample groups, however, show strong TiO_2- and iron enrichment during differentiation, distinctly different from volcanic series of island arcs which typically define more moderate Fe enrichment to negative Fe trends, and nearly flat to negative TiO_2 trends (Miyashiro 1974).

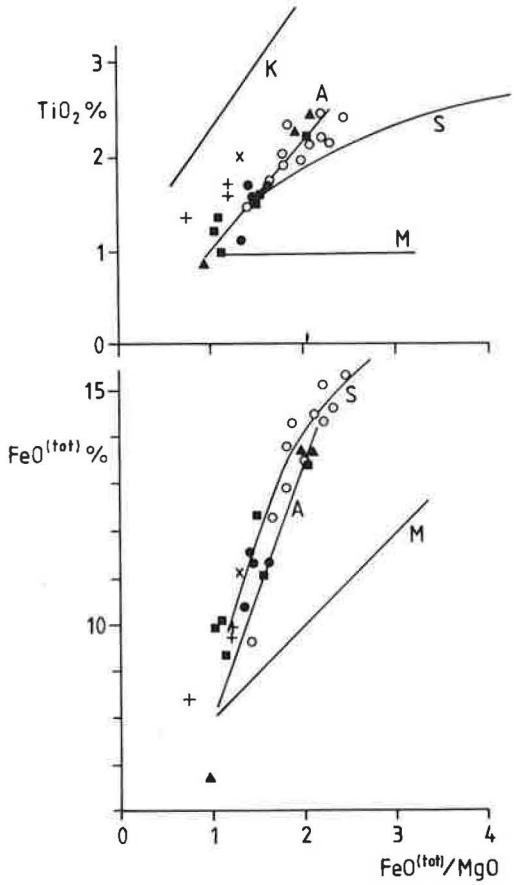

Fig. 8. TiO_2 and FeOtot vs. FeOtot/MgO plots of Resfjell and Grefstadfjell metabasalts and dykes. *Trend-lines: A* - abyssal tholeiites; *K* - Kilauea; *M* - Macauley Island (Kermadec arc); *S* - Skaergaard liquid trend. In this and subsequent figures the symbols used are as follows: ■ dykes; ● lower pillow lavas; ▲ upper pillow lavas; x dyke R 11; ○ Grefstadfjell metabasalts; + North Grefstadfjell metabasalts.

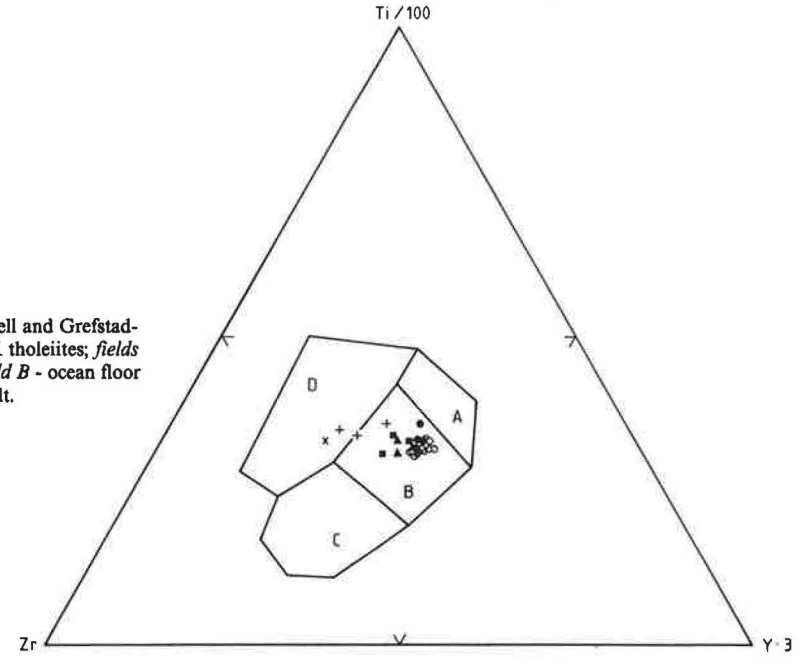

Fig. 9. Ti-Zr-Y plot of the Resfjell and Grefstadfjell rocks. *Fields A + B* - low-K tholeiites; *fields B + C* - calc-alkaline basalts; *field B* - ocean floor basalt; *field D* - within-plate basalt. Symbols as in Fig. 8.

Table 1. Major and trace element composition of rocks from Resfjell.

Sample No.	R1	R2	R3	R4	R5	R6	R7	R8	R9	R10	R11	R12	R13	R14	R15	R16	R17	R18	R19	R20
Rock type	G	G	D	D(R3)	D	D(R5)	D(R1)	D	D*	D*	D(R8)	PT	PL	PL	PL	PL*	?*	PU	PU	PU
SiO_2	46.05	48.01	49.51	49.80	48.32	47.86	47.91	46.64	49.04	35.87	44.99	50.66	50.30	47.49	49.24	48.60	49.13	48.01	49.85	47.81
Al_2O_3	23.62	15.85	13.29	15.60	14.78	13.56	16.14	15.26	13.58	11.70	15.93	14.34	13.77	14.42	13.85	13.01	12.25	12.79	12.78	18.20
Fe_2O_3	3.71	8.53	13.21	10.86	11.81	14.37	10.16	10.62	12.83	21.80	11.80	11.24	12.38	12.10	11.85	14.38	14.42	14.52	14.79	7.25
TiO_2	0.21	0.21	1.46	1.18	1.56	2.14	0.95	1.29	1.78	4.08	1.91	1.09	1.66	1.51	1.59	1.67	2.39	2.19	2.40	0.84
MgO	6.25	10.50	7.98	9.10	6.89	6.33	8.08	8.71	7.27	8.47	8.18	7.59	7.56	7.56	6.74	6.97	6.36	6.67	6.40	6.69
CaO	15.96	12.94	8.70	8.31	10.75	10.15	12.97	10.82	9.20	11.98	10.53	10.29	7.35	11.45	7.93	5.76	5.87	8.59	7.18	12.31
Na_2O	2.3	1.86	3.5	4.1	3.3	3.0	2.3	2.88	3.72	<0.20	3.08	3.4	4.0	2.86	4.1	3.8	4.4	3.66	4.7	4.0
K_2O	0.04	0.11	0.04	0.03	0.09	0.02	0.03	<0.01	<0.01	<0.01	<0.01	0.02	0.02	0.01	0.09	0.04	0.09	0.07	0.08	0.28
MnO	0.06	0.12	0.24	0.21	0.18	0.20	0.18	0.18	0.25	0.23	0.20	0.22	0.19	0.19	0.21	0.28	0.38	0.23	0.19	0.11
P_2O_5	0.04	0.02	0.10	0.09	0.12	0.15	0.06	0.13	0.15	0.20	0.18	0.07	0.10	0.14	0.12	0.11	0.19	0.21	0.18	0.07
L.O.I.	2.73	1.96	2.38	2.99	2.24	2.26	2.21	2.47	2.09	4.38	2.97	2.00	2.44	2.42	2.45	3.30	2.57	2.40	3.26	4.45
	100.97	100.11	100.41	102.27	100.04	100.04	100.99	99.01	99.92	98.92	99.78	100.92	100.17	100.15	98.17	97.92	98.05	99.34	101.81	102.01
Zr		23			92	123		92	152	106	152			94	84	80	135	134	159	
Y		8			35	45		27	33	39	27			35	35	33	52	44	52	
Sr		141			123	98		183	93	136	193			182	103	42	28	116	78	
Rb		<5			<5	<5		<5	<5	<5	<5			<5	<5	<5	<5	<5	<5	
Ba					35	22									<10	<10	<10		38	
Zn		41			88	94		82	112	74	128			76	100	89	202	102	126	
Cu		22			34	67		35	52	132	38			42	64	203	39	25	26	
Ni		150			68	56		159	102	66	125			121	66	47	39	62	51	
Cr		484			244	80		490	216	95	403			279	152	152	94	121	123	
Co					41	47									43	32	33		48	
Sc		48.4			46.2	47.6		40.4	44.5	65.2	46.7			47.4	46.8	45.9	43.1	47.3	43.8	
La					3.3	4.2		3.0	3.3	3.3	6.0			3.2	3.0	2.9	4.7	5.1	5.5	
Ce					9.3	12.0		8.5	10.0	13.0	17.2			9.3	9.3	9.3	14.5	15.5	16.6	
Nd					8.8	11.7		7.9	9.8	13.8	13.1			8.7	8.7	8.5	13.2	14.5	15.0	
Sm					3.6	4.8		3.0	4.0	5.9	4.6			3.5	3.3	3.4	5.2	5.2	5.6	
Eu					1.3	1.6		1.2	1.4	1.7	1.6			1.2	1.3	1.4	1.4	1.8	1.8	
Tb					0.77	1.03		0.66	0.96	2.57	0.94			0.83	0.88	0.88	1.27	1.20	1.35	
Yb					3.4	4.7		2.8	3.9	6.7	3.5			3.4	3.6	3.5	5.0	5.0	5.3	
Lu					0.54	0.76		0.40	0.59	0.98	0.51			0.51	0.55	0.57	0.79	0.73	0.85	
Hf		0.4			2.3	3.1		2.1	2.7	3.8	3.3			2.2	2.1	2.4	3.6	3.5	4.0	
Ta		<0.1			0.13	0.20		0.09	0.15	0.16	0.42			0.09	0.09	0.09	0.19	0.25	0.20	
Th		<0.05			0.07	0.15		0.14	0.15	<0.1	0.36			0.22	0.13	0.05	0.12	0.16	0.21	
$(Ce/Yb)_N$					0.69	0.65		0.77	0.65	0.49	1.24			0.69	0.65	0.67	0.73	0.78	0.79	
Eu/Eu*		1.09			0.99	0.90		0.07	0.92	0.73	0.97			0.92	1.0	1.05	0.70	0.93	0.85	
Th/Ta					0.5	0.8		1.6	1.0	0.6	0.9			2.4	1.4	0.6	0.6	0.6	1.1	
Ta/Yb					0.04	0.04		0.03	0.04	0.02	0.12			0.03	0.03	0.03	0.04	0.05	0.04	
Y/Zr					0.38	0.37		0.29	0.31	0.37	0.18			0.37	0.42	0.41	0.39	0.33	0.33	

G = gabbro; D = dyke; PT = pillow lava, transition zone; PL = lower pillow lava; PU = upper pillow lava;
* = samples with sulphide mineralization; ( ) = host rock intruded by dyke.

Sample localities (UTM grid reference). Map-sheets 1520 IV Trollhetta and 1521 III Løkken: R1 and R7 — 322.870; R2 — 303.882; R3 and R4 — 307.856; R5, R6 and R12 — 302.862; R8 and R11 — 305.859; R9 — 296.856; R10 — 342.855; R13 — 303.858; R14 — 306.857; R15 — 324.853; R16 and R17 — 323.853; R18 — 292.849; R19 — 329.848; R20 — 319.846.

Table 2. Major and trace element composition of rocks from Grefstadsfjell.

Sample No.	G1	G2	G3	G4	G5	G6	G7	NG1	NG2	NG3
Rock type	P	P	P	M	M	P	P	P	P	P
SiO_2	51.63	47.61	47.54	47.88	46.46	46.28	48.83	48.80	48.60	48.10
Al_2O_3	14.52	14.26	13.44	13.50	13.97	13.71	12.50	15.30	15.40	16.10
Fe_2O_3	10.31	13.03	13.69	14.25	14.72	15.05	16.18	9.00	10.40	10.50
TiO_2	1.41	1.67	1.83	1.85	1.93	2.25	2.38	1.32	1.58	1.64
MgO	6.53	7.03	6.90	6.49	7.37	7.24	6.56	11.00	7.70	7.80
CaO	8.27	9.21	9.42	8.86	10.10	7.69	7.74	6.80	8.10	8.90
Na_2O	4.27	6.65	3.64	2.51	2.40	3.68	3.57	2.96	2.80	4.00
K_2O	0.17	0.06	0.02	0.01	0.02	0.04	0.05	2.00	1.44	0.43
MnO	0.14	0.19	0.20	0.20	0.21	0.22	0.22	0.21	0.17	0.16
P_2O_5	0.10	0.12	0.13	0.14	0.14	0.17	0.18	0.08	0.11	0.14
L.O.I.	2.04	2.52	2.80	2.38	3.40	3.04	2.37	4.02	3.65	4.18
	99.39	102.35	99.61	98.07	100.72	99.37	100.58	101.49	99.95	101.95
Zr	76	91	99	101	109	133	136	91	90	117
Y	32	38	41	42	45	50	54	21	26	23
Sr	59	73	113	142	183	68	55	63	108	300
Rb	<5	<5	<5	<5	<5	<5	<5	41	17	<5
Ba	45	16	35	<10	<10	<10	<10	213	690	88
Zn	75	96	102	106	117	133	133	53	70	77
Cu	35	47	58	44	73	60	56	12	35	59
Ni	100	87	62	48	66	65	38	96	73	76
Cr	379	295	229	123	160	193	74	307	209	209
V	348	402	431	458	455	526	565			
$(La/Yb)_N$										2.0

P = pillow lava
M = massive flow (unpillowed)

Sample localities (UTM grid reference): Map-sheet 1521 II Hølonda: G1 — 413.925; G2 — 409.924; G3 — 408.922; G4 — 368.925; G5 — 410.922; G6 — 412.925; G7 — 408.922; NG1 — 372.961; NG2 — 373.959; NG3 — 372.960.

The affinity to abyssal tholeiites for the main part of the complexes is also indicated by the Ti-Y-Zr discriminant diagram of Pearce & Cann (1973), where the Resfjell and Grefstadfjell samples cluster within the field of ocean-floor basalts (Fig. 9). On the other hand, the NG metabasalts and dyke R11 straddle the OFB/ within-plate basalt field join. The samples of the upper lava member, as well as two dykes from Resfjellet (R8 and R9), are also slightly displaced from the main cluster towards the OFB/WPB field join.

The Cr-Y diagram (Fig. 10) of Pearce (1982) discriminates very clearly between mid-ocean ridge basalts (MORB) and volcanic arc basalts. Island arc tholeiites, in particular, have markedly lower Y contents and are well separated from MORB at comparable Cr values. The Resfjell and Grefstadfjell samples all plot well inside the MORB field except for a few samples which are more differentiated and fall along the lower right extension of the MORB field. Also in this diagram the NG metabasalts are distinguishable from the main trend, being displaced slightly towards lower Y values.

In Fig. 11, the Resfjell greenstones have been plotted in the Th-Ta-Hf diagram of Wood (1980). This diagram effectively discriminates between magmas formed at destructive plate margins, with characteristically high Th/Ta ratios, and those erupted at mid-ocean ridge spreading centres and within-plate settings. The latter can be subdivided, on the basis of Ta/Hf ratios, into normal (N-type) MORB, enriched (E-type) MORB and within-plate volcanites, although there is considerable overlap between E-type MORB and within-plate basalts of tholeiitic affinity (Wood 1980). Fig. 11 shows that the majority of the Resfjell samples plot in the uppermost corner of the N-type MORB field, close to the Hf apex. The only sample which is significantly different from the main cluster

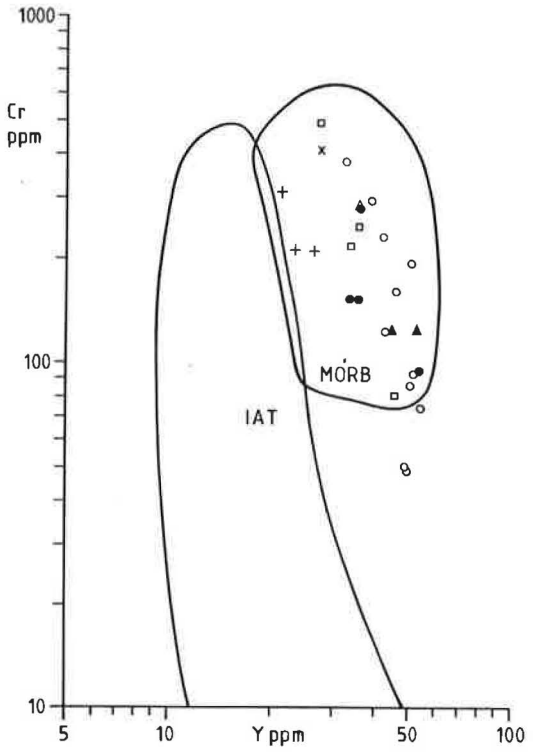

Fig. 10. Cr vs. Y plot. *Field IAT* - island arc tholeiite; *field MORB* mid-ocean ridge basalt. Symbols as in Fig. 8.

of analyses is once again the dyke R11. This is displaced towards field B in the diagram, in the area of overlap between N-type and E-type MORB. The slight spread towards the Th apex for the other samples, causing one lower pillow lava analysis to plot just within the field of island arc tholeiites, is not considered significant. Most of the samples have levels of Ta, and particularly Th, which are extremely low and close to normal detection limits, resulting in possible large relative errors. Indeed, control analysis using GSP-1 as standard suggests that such errors, especially in Th values, may in some cases be important in Th-Ta-Hf discrimination of material which is low in these elements. Additionally, the effect of alteration during secondary processes will be most crucial to rocks like these, with very low contents of Th and Ta. Although Th is generally considered to be fairly stable, possible Th mobility is mentioned by Wood et al. (1979). Such mobility would of course contribute to variations in Th/Hf and Th/Ta ratios, in addition to the variation related to analytical uncertainties. In this respect it is noteworthy that the sample which is most affected by hydrothermal alteration (R10) is the one having the lowest Th/Hf ratio (<0.03), although the analytical significance of this can perhaps be disputed.

A frequently used method of comparing the chemical composition of various rocks is a normalizing procedure using, for instance, an 'average MORB' composition as reference (Pearce 1982). This is shown in Fig. 12. Because of uncertainties connected with possible alteration, we have omitted the 'large ionic lithophile' (LIL) elements from the diagram. In Fig. 12A, where average values for various rock types are compared, the most striking feature is the general similarity of the dykes (excluding sample R11) and lower and upper pillow lavas to average MORB, although the upper pillow lavas seem to be somewhat more evolved than average MORB. The comparatively low Cr, particularly in the upper lavas, is also related to the somewhat fractionated nature of these 'average' rocks. The obvious depletion of the most incompatible and stable elements Th and Ta compared to the other elements of the series is thought to reflect a primary feature of the magmas. Irregularities in the lower pillow lava pattern for Th and especially Ta can possibly be ascribed to the large analytical errors for these rocks which have the lowest concentrations of Th and Ta (see above).

The dyke R11 shows a normalized geochemical pattern markedly different to those described above. The most incompatible of the stable elements, Th and Ta are enriched by a factor of approximately 2 compared with 'normal MORB'. The pattern from Ce towards Yb (or Y) describes a gentle slope from this enrichment, consistent also with the REE pattern (Fig. 15). A normalized pattern like this can be found in tholeiitic basalts of within-plate affinity, and in mid-ocean ridge basalts with compositions transitional to E-type MORB (Fig. 12B). In this diagram most within-plate tholeiites show about the same relative enrichment of the elements Zr-Hf-Sm-Ti, with a steep gradient down to the more depleted Y and Yb, whereas transitional to E-type MORB describe smoother patterns (Pearce 1982). In this regard, dyke R11 (and the related NG metabasalts) is transitional between the two types. The slight negative Y anomaly seen in the R11 pattern may suggest that this Y value is somewhat too low; however, if this is so, then dyke R11 (and the NG metabasalts) is most akin to transitional MORB's.

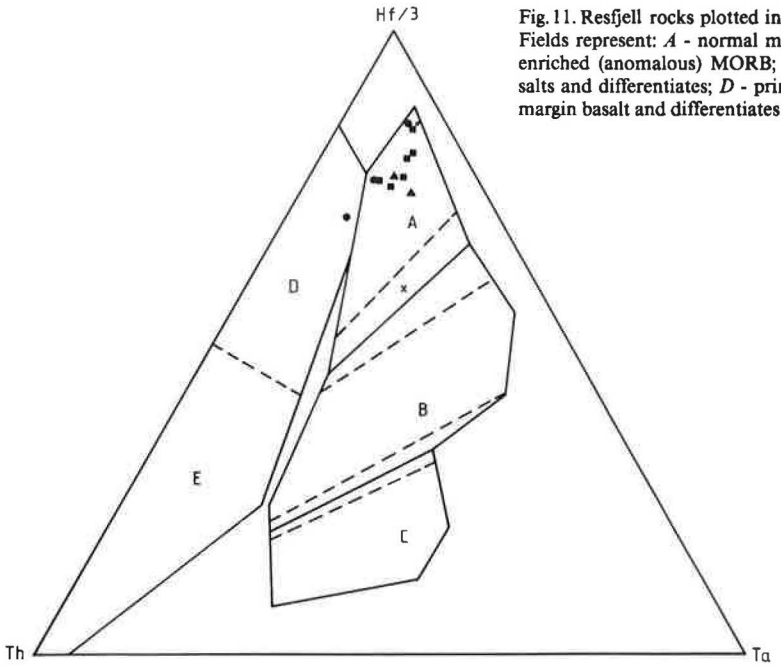

Fig. 11. Resfjell rocks plotted in the Th - Hf/3 - Ta ternary diagram. Fields represent: *A* - normal mid-ocean ridge basalt (MORB); *B* - enriched (anomalous) MORB; *C* - alkaline within-plate basalts and differentiates; *D* - primitive arc tholeiite; *E* - destructive margin basalt and differentiates (calc-alkaline). Symbols as in Fig. 8.

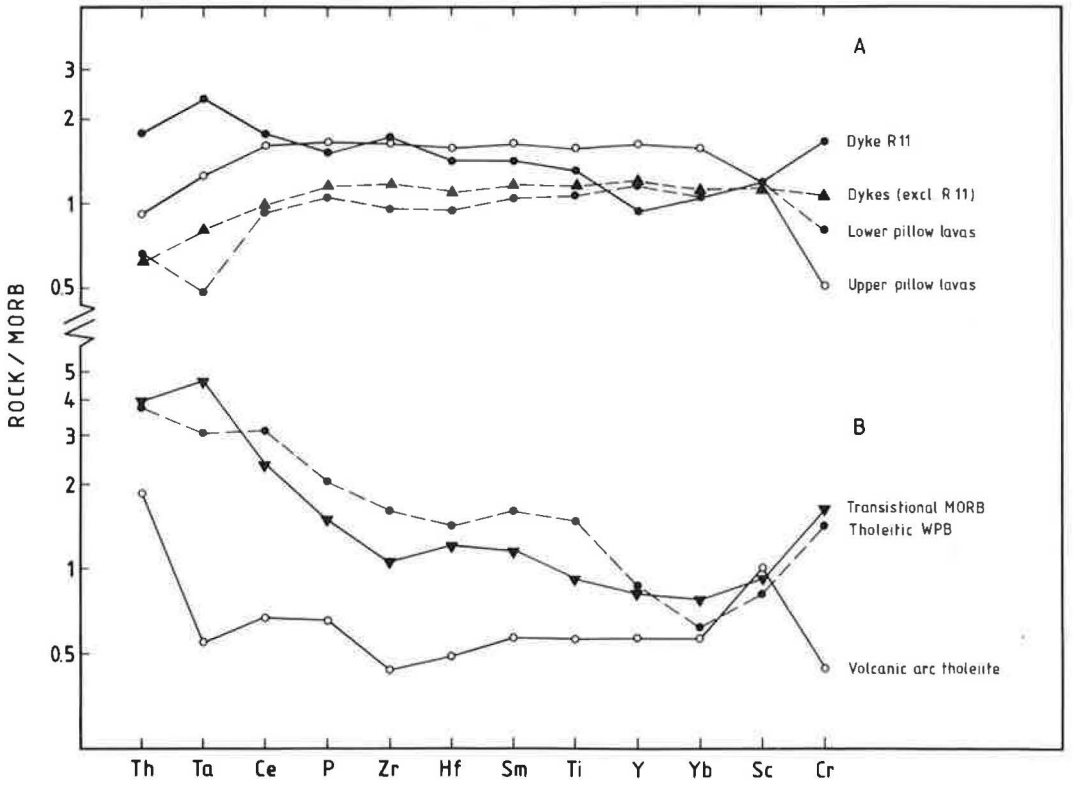

Fig. 12. MORB-normalised trace element patterns of Resfjell rocks (A) and recent volcanic rocks of three types of tectonic setting (B).

Discussion

The presentation above has demonstrated two obvious characteristics:

a) The main lithologies in the Resfjell and Grefstadfjell complexes are very similar to each other and show geochemical signatures typical of ocean floor basalts.
b) In both areas there are a few rocks which deviate from this pattern (dyke R11 in Resfjell and the NG metabasalts from Grefstadfjell).

On the basis of the general similarity demonstrated above, the geochemistry and petrology of rocks from the two areas will be discussed together, although such an approach obviously has serious limitations (mainly related to their different geographical locations). These problems raise questions of the following type: (i) Is it likely that rocks from the two separate areas may represent the same or similar mantle source? (ii) Can rocks from the two areas be treated as representing members related to each other by fractional crystallization of a certain type of primary magma? (iii) Are the geochemical variations observed related to processes other than fractional crystallization, e.g. such as different degrees of partial melting, mixing between primary and evolved magmas, etc.?

The analytical data presented here do not give definite answers to these questions. However, in the discussion below we have chosen to base the main comments on fractional crystallization because this process would seem to have been important. In fact, the presence of cumulate type leucogabbro within the lower stratigraphical part of the Resfjell ophiolite fragment is a mineralogical (as opposed to chemical) manifestation that fractional processes operated in the Resfjell magma system. The contribution of other factors in the development of these two rock series will also be discussed.

In the discussion below, Zr is chosen as a differentiation index because of its incompatible nature at low and intermediate SiO_2 levels. Furthermore, zirconium is stable during secondary alteration processes (Pearce & Cann 1973), and therefore probably one of the most reliable fractionation indices available for low-grade metamorphic volcanites.

In Fig. 13, the stable elements TiO_2, P_2O_5, and Y are plotted against Zr for the rocks in the Resfjell and Grefstadfjell areas. In the TiO_2-Zr diagram, the majority of samples define a very clear trend of strong TiO_2 enrichment almost throughout the series. Assuming that the bulk partition coefficient for Zr was between 0.01 and 0.1 (Wood et al. 1979, Pearce & Norry 1979), a bulk partition coefficient for titanium of between 0.16 and 0.23 can be estimated from a visual best fit line. This suggests that significant crystallization of magnetite or other Fe-Ti oxides did *not* occur in the parent magmas to these rocks, except in the very late stages. This is corroborated by the strong correlation between Zr and V (not shown), which also is partitioned into magnetite (Leeman et al. 1978). Assuming Rayleigh fractionation with Zr as the incompatible element (cf. Allégre et al. 1977), it can be calculated from the TiO_2-Zr data that probably as much as 55% or more of the melt was crystallized before Fe-Ti oxides started to precipitate in the late stages of differentiation, as seen from the sudden drop in TiO_2 at values of Zr between 170—190 ppm (Fig. 13). The dyke R11 and the NG metabasalts define a trend significantly different from the main group of samples, with higher Zr at similar TiO_2 values. Another dyke sample from Resfjellet (R8) also falls close to this trend.

The P_2O_5 and Y vs Zr diagrams (Fig. 13) reveal that apatite was virtually absent from the crystallizing assemblage through the whole series of analysed dykes and metavolcanites; a bulk partition coefficient of 0.05 or less is estimated from the data. The corresponding value for Y is 0.09—0.18. The higher coefficients for Y may be ascribed to its partitioning into fractionating pyroxene. Like the TiO_2 vs Zr diagram, the Y-Zr data suggest the existence of two or more types of magma describing different trends in the variation diagrams. Here, the majority of the Grefstadfjell samples, together with the lower pillow lavas and dykes in the Resfjell area, form a well-defined trend with a Y/Zr ratio of about 0.4. Using the Rayleigh distillation law, it can be calculated that up to 80% crystallization was required to form the most evolved of these effusives, assuming that the apparently aphyric metabasalts with the lowest Zr, TiO_2, Y and P_2O_5 contents are close to the composition of the parent magma. The NG metabasalts and the Resfjell dyke R11 are clearly different from this trend, with considerably lower Y/Zr ratios (about 0.2), while the Resfjell upper pillow lavas and two dykes (R8 and R9) fall between the two extremes.

The Al_2O_3 vs TiO_2 diagram (Fig. 14) demonstrates a marked negative correlation between

Al_2O_3 and the degree of fractionation (only samples within the TiO_2 enrichment part of the TiO_2-Zr trend of Fig. 13 are included). A loss of Al_2O_3 from about 16% in the most primitive samples, to about 12% in the most fractionated rocks (which represent approximately 30—40% residual liquid) suggests that plagioclase must have been a major phase throughout the crystallization history of these magmas. A semi-quantitative calculation based on 4% Al_2O_3 loss at 30% residual liquid gives a weight proportion of about 25% basic plagioclase in the crystallizing assemblage. Lower and upper pillow lavas as well as dykes follow this trend; however, the north Grefstadfjell samples and dyke R11 apparently define a flatter trend possibly indicating less significant plagioclase crystallization. One upper pillow lava from Resfjellet (R20) is apparently enriched in Al_2O_3 (18.2%) compared with the general trend. The same sample is enriched in CaO and is low in iron and MgO compared to the FeO/MgO ratio (Table 1 and Fig. 8), consistent with a significant proportion of cumulate basic plagioclase in this upper pillow basalt. The steep negative trends of Cr and Ni with fractionation (Fig. 10; Tables 1 & 2) suggest that clinopyroxene, olivine or Cr-spinel were crystallizing together with plagioclase. Although only an estimate of the clinopyroxene/olivine proportions can be obtained from the data on these metamorphosed rocks, the variation of Sc suggests significant clinopyroxene crystallization. Sc is slightly depleted during differentiation of the present rocks, indicating a bulk partition coefficient of between 1.1 and 1.5 and thus a weight proportion of 55—75% clinopyroxene in the crystallizing assemblage based on a D_{Sc}^{Cpx} of 2 (Baker et al. 1977).

The chondrite-normalized rare earth element (REE)-patterns of the Resfjellet rocks (Fig. 15) show only small variations. Both lower and upper pillow lavas are depleted in the light REE (LREE). The patterns are essentially parallel; however, a slight increase in the Ce/Yb normalized ratios in the upper lavas (0.78—0.79) compared with the lower ones (0.65—0.69) may suggest that the two are not directly related by simple fractional crystallization. The same LREE-depleted patterns are shown by most of the dykes, with $(Ce/Yb)_N$ ratios between 0.65 and 0.77 in the lavas. Among the non-mineralized samples, dyke R11 is a notable exception, having a flat or slightly LREE-enriched pattern with a $(Ce/Yb)_N$ ratio of 1.24. Some dykes have higher Sm/Tb ratios than those in the smooth

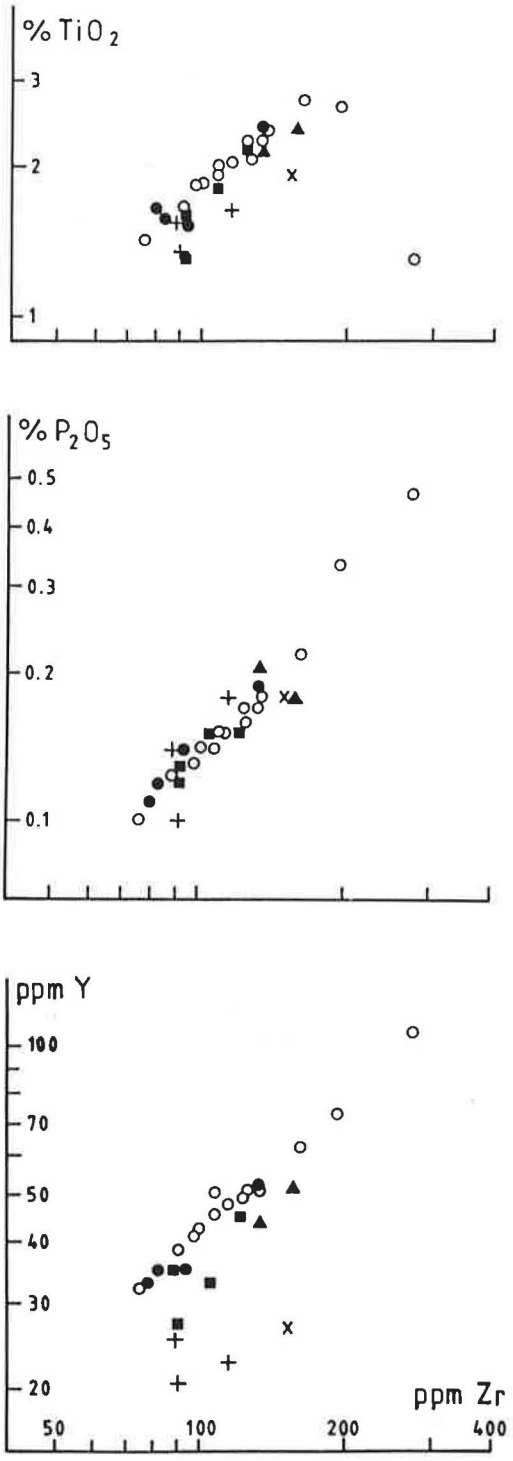

Fig. 13. TiO_2/Zr, P_2O_5/Zr and Y/Zr variation diagrams for Resfjell and Grefstadfjell metabasaltic lavas and dykes. Symbols as in Fig. 8.

patterns of the pillow lavas; however, repeated analyses (using GSP-1 as standard) have shown that these variations are not real. The analysed leucogabbro (R2) has very low contents of REE, consistent with its low abundances of other incompatible elements (Table 1) and similar to what is found in other ophiolite gabbros (e.g. Prestvik 1980). The LREE-depleted pattern clearly reveals its relationship to the lavas and majority of the dykes. The gabbro also shows a minor positive Eu anomaly consistent with its high content of probable cumulate plagioclase. The generally increasing negative Eu anomaly, among non-mineralized samples, with Eu/Eu* from around 1 in the most primitive dykes and lavas, to 0.85 in the most evolved upper pillow lavas (Table 1) is compatible with fractionation of plagioclase.

Dyke sample R10, which is mineralized, shows a geochemistry which is here interpreted as the result of alteration (Table 1). It is the only one of the mineralized samples where the overall REE pattern is significantly different compared with the others (Fig. 15). Here, the LREE are preferentially lost from the rock, giving a $(Ce/Yb)_N$ ratio as low as 0.49. However, Eu is the element that has been most susceptible to loss during the alteration processes that accompanied mineralization. Both R10 and the considerably less altered greenstone R17 have negative Eu anomalies of 0.70—0.73, and a slight loss of Eu can probably be detected in the slightly altered dyke R9, which otherwise has a quite normal chemical composition (Table 1). On the other hand, Eu shows no significant depletion in one mineralized pillow lava sample (R16) which is more affected in, for instance, its CaO, Sr and total iron contents by alteration than samples R17 and R9. The apparent inconsistent behaviour of Eu and Sr in these rocks may be related to different Eh conditions during the mineralizing process; such that Eu in some cases is kept in the Eu^{3+} state, which is not as susceptible to leaching as the more readily soluble Eu^{2+} (similar to Sr^{2+} (Henderson 1984)).

Petrogenetic and geotectonic significance

There is a striking similarity between the igneous rocks from the Resfjell and Grefstadfjell complexes. The resemblance is most prominent in lower to middle parts of the volcanic sequences, where the metabasalts cover virtually identical compositional ranges with quite similar

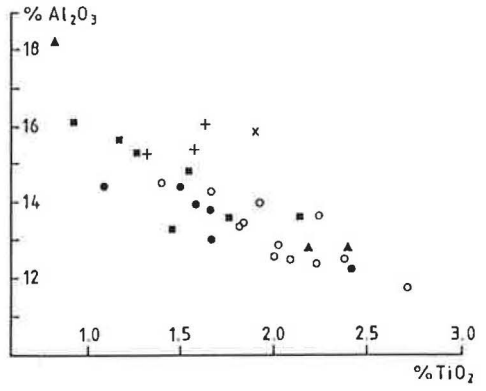

Fig. 14. Al_2O_3 vs. TiO_2 diagram for the Resfjell and Grefstadfjell rocks. Symbols as in Fig. 8.

element abundances and ratios. Alkali-SiO_2 relations as well as low Ta and Th values and LREE-depleted patterns clearly reveal that these metavolcanites were originally of typical tholeiitic nature. The TiO_2 and FeO(tot.)vs. FeO(tot.)/-MgO diagrams (Fig. 8) show that the differentiation trends are different from subduction-related lava series, and their similarity to MORB is well demonstrated here and in several other discrimination diagrams.

Furthermore, the low abundances of the most incompatible elements Ta and Th (and possibly also the mobile elements Ba, Rb and K_2O) compared with the less incompatible elements (Fig. 12) classify the metabasalts as highly depleted N-type MORB. Such rocks are commonly considered to reflect previous depletion of the mantle source by earlier melting events (Gast 1968, Wood 1979).

The individual lava flows in these lower, main parts of the sequences have compositions which are evidently strongly controlled by extensive fractional crystallization processes, although they are all in the basaltic range (Table 1). The main effects of this are large ranges of stable incompatible elements with near proportional inter-element variations, strong iron enrichment coupled with a moderate depletion of MgO and Al_2O_3, and a marked loss of Cr and Ni towards the most evolved metabasalts. These variations can apparently be interpreted semi-quantitatively in terms of up to more than 70% total fractional crystallization of an assemblage consisting of more than 50% clinopyroxene, some 25% plagioclase and less olivine (or larger amounts of orthopyroxene?), with crystallization of a Ti-bearing phase (mt?) only in the latest stage of differentiation. At oceanic sprea-

ding axes such extensive fractionation is characteristic of relatively fast-spreading plate boundaries (Nisbet & Fowler 1978, Pearce & Norry 1979), and may relate to mixing of upflowing primitive magma with evolved melts formed by crystallization in large magma chambers (open system fractionation). Periodic tapping of various parts of such chambers may give basalt compositions ranging from the primitive parent magma to highly fractionated ferrobasalts enriched in Zr, Y, REE, etc. (Prestvik 1985).

Data on multiple intrusions of dykes that can be related to the lower pillow lavas in Resfjellet (Table 1, R3-R6) are consistent with such a process: very primitive dykes may intrude more fractionated ones, whereas in other places highly evolved dykes cut through less fractionated intrusions. The upper pillow lavas of the Resfjell area cover essentially the same range of chemical compositions as found in the lower lavas, although field evidence suggest that highly evolved (now dark greenish, stilpnomelane-bearing) flows are more prominent in this upper part of the sequence. Just as the lower lavas, these metabasalts are strongly tholeiitic with LREE-depleted patterns and follow most of the variation trends described in the former. A notable difference, however, is a somewhat lower Y/Zr ratio as well as a slightly lower TiO_2/Zr in the upper lavas (Fig. 13). Two of the analysed dykes (R8 and R9) can be related to this part of the volcanic pile.

The upper lavas and related dykes (excluding dyke R9 which is mineralized and slightly altered and thus may have lost some of its original LREE content) also have higher $(Ce/Yb)_N$ ratios (0.77—0.79) than the lower lavas and associated dykes (0.65—0.69 for the non-mineralized samples). The differences are, however, too small to move the rocks outside the compositional fields of normal mid-ocean ridge basalts in any of the discriminant diagrams. In accordance with the differences mentioned above, the overall composition of the upper lavas shows a flatter and more evolved MORB-normalized pattern (Fig. 12). It is tentatively suggested, therefore, that the magmas feeding the upper lavas formed from the same type of mantle source, but represent a slightly smaller degree of partial melting. This melt was compositionally modified, by extensive fractional cryctallization in magma chambers, similar to the lower pillow lavas. A possible link between the upper lavas and the high-level, plagioclase-rich leucogabbros is indicated by the abundance of cumulate plagioclase in one flow (R20). Field evidence suggests that chemically similar, strongly plagioclase-phyric dykes (e.g. R7) are petrogenetically related to these gabbros, which intrude and are later than the lower pillow lavas. A similar link between the upper lavas and the microgabbros cannot be confirmed geochemically. However, intrusion relationships indicate that the microgabbros were intruded only shortly after the high-level emplacement of the partly crystallized, plagioclase-rich leucogabbros. Furthermore, presence of apatite and Fe-Ti oxides in the microgabbros indicates a relatively evolved composition compatible with the commonly fractionated nature of the upper pillow lavas.

The last recorded magmatic phase is that represented by the north Grefstadfjell metabasalts and one of the analysed dykes (R11) in the Resfjell ophiolite complex; the latter intrudes a dyke (R8) which is chemically relatable to the upper pillow lavas. Quite contrary to the rest of the suite, these rocks are enriched in the most incompatible elements relative to normal MORB (Fig. 12). Th-Ta-Hf and Ta/Yb ratios in sample R11 (Fig. 11 and Table 1), as well as the overall chemistry, tend to classify these rocks as T-type (transitional type) MORB, similar to those found on some anomalous spreading ridge segments and possibly derived from primitive or relatively undepleted mantle sources (cf. Erlank & Kable 1976). The upper lavas of the Resfjell ophiolite fall intermediate between these rocks and the lower lavas.

The geochemical data presented above show that no component of subduction-related magmatism can be traced in the inter-element ratios or element variations/abundances of the Resfjell and Grefstadfjell ophiolite sequences. In particular, this is demonstrated by strong iron and TiO_2 enrichment trends, relatively high contents of TiO_2, Zr, Y etc. at high Cr values, and by the relatively low Th/Ta ratios. It has been argued by Roberts et al. (1984), mainly on the basis of lithostratigraphic considerations, that the ophiolites of the western Trondheim district (except the Støren *sensu stricto* greenstones) formed in a marginal basin rather than at a major ocean spreading ridge. Typical subduction-related metavolcanites do indeed occur higher up in the overlying, mixed sedimentary-volcanic sequences of the Lower and Upper Hovin Groups (Roberts et al. 1984). The precise temporal relationship between the Resfjell and Grefstadfjell ophiolites and the slightly younger

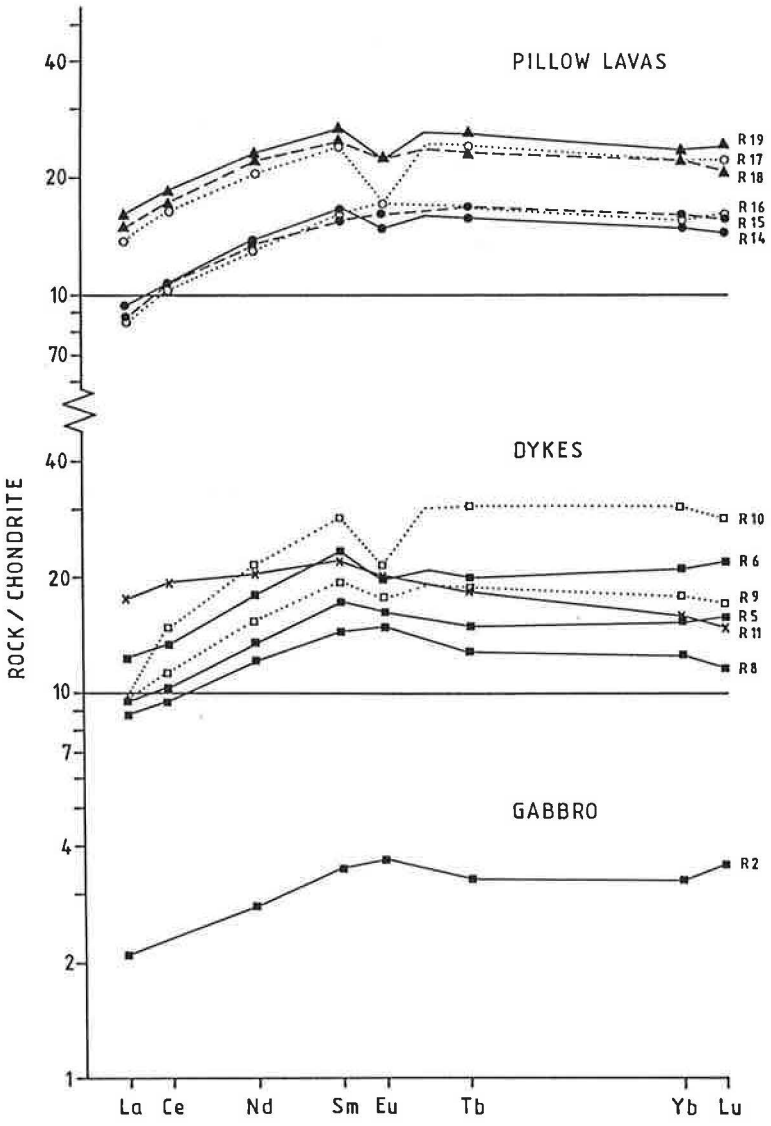

Fig. 15. Chondrite-normalised REE patterns of Resfjell gabbro, dykes and pillow lavas.

sequences is, however, somewhat ambiguous in view of the lack of precise dating of the former, as stressed by Grenne (1986). The present geochemical data cannot be taken to support the back-arc marginal basin hypothesis for the Resfjell and Grefstadfjell ophiolites, as most recent marginal basin basalts, as well as the 'supra-subduction zone ophiolites' of Pearce et al. (1984), show some influence of subduction-zone magma characteristics, in particular a higher large-ionic lithopile (LIL) element/high field strength (HFS) element ratio (e.g. Th/Ta — cf. Saunders & Tarney 1984). However, it is shown by Saunders & Tarney (1984) that basalts indistinguishable from N-type MORB may be erupted in extensional basin settings during the earliest stages of subduction systems, before the underlying mantle wedge has become significantly enriched in the mobile LIL elements that are driven off the dehydrating subducting oceanic crust (e.g. Saunders et al. 1980). Basalts resembling E-type or T-type MORB may also occur locally in such settings. Thus, the Resfjell—Grefstadfjell data are neither indicati-

ve of, nor contradictory to, a marginal basin origin for these ophiolites. It is likely though, that, if they were related to subduction, the spreading took place very early in the subduction process, above a normal depleted or primitive suboceanic mantle wedge, or possibly in a very wide back-arc marginal basin.

Paleotectonic reconstruction

The Resfjell complex exhibits an outcrop picture (Plate 1) comprising an ideal cross-section through characteristic parts of the original ocean floor of which it was once composed. Based on the field data, an interpreted schematic cross section is presented i Fig. 3.

A conspicuous feature of the Resfjell ophiolite complex is a marked unconformity (Fig. 3) between the lower and upper lava members, at least in the central and eastern areas (Plate 1). There, the dykes cut at near-right angles to the E-W to ENE-WSW striking paleo-horizontal plane, which is well defined in this part of the sequence by abundant drained pillows with internal lava shelves. Igneous layering, pillow breccia units and extensive jasper horizons in the upper lava member, by contrast, strike E-W to ESE-WNW. It has been argued above that the contact between the two members is primary and not tectonic; metadolerite dyke swarms appear to be continuous from the lower to the upper lavas. At least two modes of formation can thus be considered:

1. *The sea-floor crust may have been extensively faulted and accompanied by considerable tilting of the individual fault blocks.*

Tilting of fault blocks due to crustal extension is common at oceanic spreading axes, particularly at relatively *low* spreading rates (Allmendinger & Riis 1979). This interpretation would imply that the Resfjell rocks probably moved from a spreading centre which was situated — in the present inverted position — west of the complex, assuming backtilting from a central axis with fault planes dipping towards the axis (cf. Ballard & Moore 1977). However, although such processes are indeed likely in an extensional environment, they would result in a very steep sea-floor relief with subsequent deposition of coarse talus adjacent to the fault scarps (Ballard & Moore 1977), and such breccias are not at all characteristic of the contact between the lower and upper lava members of the Resfjell ophiolite. Furthermore, the geochemical data discussed above indicate a fast spreading situation for the Resfjell metabasalts.

2. *The sea-floor crust was uplifted and partly eroded subsequent to formation of the lower pillow lavas.*

The occurrence of exotic clasts of felsic igneous rocks in the sediments which rest on parts of the Resfjell lower pillow lava surface, are more consistent with this interpretation. In this regard, it can be noted that rhyodacitic metavolcanites of probable subduction affinity are locally interbedded with tholeiitic metabasalts west and northwest of Løkken, c. 15 km north of Resfjell (Grenne in prep.), and that sequence can apparently be correlated with the upper volcanic member of the Løkken ophiolite fragment. It seems likely, therefore, that the ophiolitic crust was, at least partly, uplifted and eroded in the north/northwest and contributed detritus to the sediments within the Resfjell ophiolite, where tension-related volcanism was still active. If, as suggested above, the Resfjell lower lavas were subject to some erosion prior to eruption of the comparable MORB-type upper lavas (with a common mantle source for the lower and upper lava members) and the penecontemporaneous sedimentation, it implies a very unstable geotectonic setting quite different from that of a normal oceanic spreading ridge situation. The balance of evidence thus points to formation of the Resfjell—Grefstadfjell ophiolites in a marginal basin, or possibly a fore-arc setting, even though there is no detectable subduction component in the geochemistry of the igneous rocks. At the present stage of knowledge, no definite explanation can be given for this apparent discrepancy. Possible, although somewhat speculative, models may include crustal extension above newly subducted oceanic crust during the initial stages of subduction (cf. Pearce et al. 1984) or, alternatively, sea-floor spreading in a very wide marginal basin (cf. Saunders & Tarney 1984). Both are 'supra-subduction' settings in which MORB-type magmas may have been produced.

Acknowledgements

The fieldwork for this project was sponsored by Orkla Industrier A/S, Løkken. We are especially grateful for the help and enthusiasm given by Mr. Gudmund Grammeltvedt. The first draft of the manuscript was reviewed by Drs. Stephen Lippard and Harald Furnes. The present manuscript benefitted considerably from their constructive criticism and suggestions.

Contribution No. 26 to NAVF's International Lithosphere Program (ILP).

References

Allégre, C.J., Treuil, M., Minster, J.F., Minster, B. & Albaréde, F. 1977: Systematic use of trace elements in igneous processes. Part I: Fractional crystallization processes in volcanic suites: *Contrib. Miner. Petrol. 60,* 57—75.

Allmendinger, R.W. & Riis, F. 1979: The Galapagos Rift at 86°W: 1. Regional morphological and structural analysis. *Geophys. Res., 84,* 5379—5389.

Baker, B.H., Goles, G.G., Leeman, W.P. & Lindstrøm, M.M. 1979: Geochemistry and petrogenesis of a basalt-benmoreite-trachyte suite from the southern part of th Gregory Rift, Kenya. *Contrib. Miner. Petrol. 64,* 303—332.

Ballard, R.D. & Moore, J.G. 1977: *Photographic atlas of the Mid-Atlantic Ridge rift valley.* Springer Verlag, 114 pp.

Ballard, R.D., Holcomb, R.T. & van Andel, T.H. 1979: The Galapagos rift at 86°W: 3. Sheet flows, collapse pits, and lava lakes of the rift valley. *J. Geophys. Res. 84,* 5407—5422.

Chaloupsky, J. 1970: Geology of the Hølonda—Hulsjøen area, Trondheim region. *Nor. geol. unders. 266,* 277—304.

Chaloupsky, J. 1977: Map sheet Hølonda 1—50 000. *Nor. geol. unders.*

Erlank, A.J. & Kable, E.J.D. 1976: The significance of incompatible elements in mid-Atlantic ridge basalts from 45°N with particular reference to Zr/Nb. *Contrib. Miner. Petrol. 54,* 281—191.

Flanagan, F.J. 1973: 1972-values for international geochemical reference standards. *Geochim. Cosmochim. Acta 37,* 1189—1200.

Furnes, H., Roberts, D., Sturt, B.A., Thon, A. & Gale, G.H. 1980: Ophiolite fragments in the Scandinavian Caledonides. *In* Panayiotou, A. (ed.): Proc. Int. Ophilite Symp. Cyprus 1979, 582—600.

Gale, G.H. & Roberts, D. 1974: Trace element geochemistry of Norwegian Lower Paleozoic basic volcanics and its tectonic implications. *Earth Planet. Sci. Lett. 22,* 380—390.

Gast, P.W. 1968: Trace element fractionation and the origin of tholeiitic and alkaline magma types. *Geochim. Cosmochim. Acta 32,* 1057—1086.

Gee, D.G., Guezou, J.-C., Roberts, D. & Wolff, F.C. 1985: The central-southern part of the Scandinavian Caledonides. *In* Gee, D.G. & Sturt, B.A. (eds.): The Caledonide Orogen — Scandinavia and Related Areas, pp. 109—133. J. Wiley & Sons Ltd, Chichester.

Grenne, T. 1979: Vassfjellet — et underpaleozoisk ofiolittfragment i det vestlige Trondheimsfelt (abstract). *Geologynytt 13,* p. 24.

Grenne, T. 1986: Ophiolite-hosted Cu-Zn-deposits at Løkken and Høydal, Trondheim nappe complex, upper allochthon. *In* Stephens, M.B. (ed): Stratabound mineralizations in the central Scandinavian Caledonides. Excursion Guide 2, 7th IAGOD Symp. Luleå, *Sver. Geol. Unders., Ser. Ca, No. 60,* pp. 55—65.

Grenne, T. & Roberts, D. 1981: Fragmented ophiolitic sequences in Trøndelag, Central Norway. Uppsala Caledonide Symposium 1981; excursion guide B 12, 40 p.

Grenne, T. & Roberts, D. 1983: Volcanostratigraphy and eruptive products of the Jonsvatn Greenstone Formation, Central Norwegian Caledonides. *Nor. geol. unders. 387,* 21—38.

Grenne, T., Grammeltvedt, G. & Vokes, F.M. 1980: Cyprus-type sulphide deposits in the western Trondheim district, central Norwegian Caledonides. *In* Panayiotou, A. (ed): Proc. Int. Ophiolite Symp., Cyprus 1979, 727—743.

Guezou, J.-C. 1981: Geologisk kart over Norge, berggrunnskart 1:250 000, foreløpig utgave. *Nor. geol. unders.*

Heim, M. 1984: The Resfjell ophiolite fragment (Trondheim Nappe Complex). *In* Armands & Schager (eds.): Abstracts from 16. Nordiska Geologiska Vintermötet. *Meddel. Stockh. Univ. Geol. Inst. 255,* p. 86.

Henderson, P. 1984: General geochemical properties and abundances of the rare earth elements. *In* Henderson, P. (ed.): Rare earth element geochemistry. Elsevier. pp. 1—32.

Irvine, T.N. & Baragar, W.R.A. 1971: A guide to the chemical classification of the common volcanic rocks. *Can. J. Earth Sci. 8,* 523—548.

Kjeldsen, S. 1984: *En undersøkelse av sulfidmineraliseringer i Grefstadfjell og Resfjellområdene, Løkkenfeltet.* Unpubl. thesis, NTH, Trondheim, 136 pp.

Miyashiro, A. 1975: Classification, characteristics and origin of ophiolites. *J. Geol. 83,* 249—281.

Mottl, M.J. 1983: Metabasalts, axial hot springs, and the structure of hydrothermal systems at mid-ocean ridges. *Geol. Soc. Am. Bull., 94,* 161—180.

Nisbet, E.G. & Fowler, C.M.R. 1978: The mid-Atlantic ridge at 37 and 45 N: some geophysical and petrological constraints. *Geophys. J. Roy. Astron. Soc., 54,* 631—660.

Oftedahl, C. 1980: Geology of Norway. *Nor. geol. unders. 256,* 3—114.

Oftedahl, C. 1981: *Norges Geologi.* En oversikt over Norges regionalgeologi, 2. utgave. Tapir, Trondheim. 207 pp.

Oftedahl, C. & Prestvik, T. 1985: Continental margin pyroclastics and the stratigraphy of the 'Horg Syncline'. *Rep. 22, Geol. Inst. NTH, Trondheim,* 1—22.

Pearce, J.A. 1976: Statistical analysis of major element patterns in basalts. *J. Petrol. 17,* 15—43.

Pearce, J.A. 1982: Trace element characteristics of lavas from destructive plate boundaries. *In* Thorpe, R.S. (ed.): Andesites. John Wiley & Sons, London, 525—548.

Pearce, J.A. & Cann, J.R. 1973: Tectonic setting of basic volcanic rocks determined using trace element analyses. *Earth Planet. Sci. Lett. 19,* 290—300.

Pearce, J.A. & Norry, M.J. 1979: Petrogenic implications of Ti, Zr, Y and Nb varations in volcanic rocks. *Contrib. Miner. Petrol. 69,* 33—47.

Pearce, J.A., Lippard, S.J. & Roberts, S. 1984: Characteristics and tectonic significance of supra-subduction zone ophiolites. *In* Kokelaar, B.P. & Howells, M.F. (eds.): Marginal basin geology. *Geol. Soc. Spec. Publ. No. 16,* 77—94.

Prestvik, T. 1980: The Caledonian ophiolite complex of Leka, north-central Norway. *In* Panayiotou, A. (ed.): Proc. Int. Ophiolite Symp. Cyprus 1979, 555—566.

Prestvik, T. 1985: Petrology of Quaternary volcanic rocks from Öræfi, southeast Iceland. *Rep. 21, Geol. Inst., NTH, Trondheim,* 1—81.

Roberts. D. 1978: Caledonides of south central Norway. *In* Tozer, E.T. & Schenk, P. (eds.): Caledonian — Appalachian Orogen of the North Atlantic Region. *Geol. Surv. Canada Paper 78—13,* 31—37.

Roberts. D. 1980: Petrochemistry and palaeogeographic setting of the Ordovician volcanic rocks of Smøla, central Norway. *Nor. geol. unders. 359,* 43—60.

Roberts, D. & Wolff, F.C. 1981: Tectonostratigraphic development of the Trondheim region Caledonides, central Norway. *J. Struc. Geol. 3,* 487—494.

Roberts, D., Grenne, T. & Ryan, P.D. 1984: Ordovician marginal basin development in the central Norwegian Caledonides. *In* Kokelaar, B.P. & Howells, M.F. (eds.): Marginal basin geology. *Geol. Soc. Spec. Publ. No. 16,* 233—244.

Rosencrantz, E. 1983: The structure of sheeted dikes and associated rocks in North Arm massif, Bay of Islands ophiolite complex, and the intrusive process at oceanic spreading centers. *Can. J. Earth Sci., 20,* 787—801.

Ryan, P.D., Skevington, D. & Williams, D.M. 1980: A revised interpretation of the Ordovician stratigraphy of Sør-Trøndelag and its implications for the evolution of the Scandinavian Caledonides. Proc. IGCP Cal. Orogen Symp. — *Virginia Poly. Inst. & State Univ. Memoir 2,* 99—103.

Sand, K. 1986: A study of Paleozoic iron—formations in the central Norwegian Caledonides. *Rep. 23b, Geol. Inst. NTH, Trondheim,* 23 pp.

Saunders, A.D. & Tarney, J. 1984: Geochemical characteristics of basaltic volcanism within back-arc basins. *In* Kokelaar, B.P. & Howells, M.F. (eds.): Marginal basin geology. *Geol. Soc. Spec. Publ. No. 16,* 59—76.

Saunders, A.D., Tarney, J. & Weaver, S.D. 1980: Transverse geochemical variations across the Antarctic Peninsula: implications for the genesis of calc-alkaline magmas. *Earth Planet. Sci. Lett. 46,* 344—360.

Vogt, T. 1945: The geology of part of the Hølonda-Horg district, a type area in the Trondheim region. *Nor. Geol. Tidsskr. 25,* 449—528.

Wolff, F.C. 1976: Geologisk kart over Norge, berggrunnskart Trondheim, 1:250.000. *Nor. geol. unders.*

Wolff, F.C. 1979: Beskrivelse til de berggrunnsgeologiske kart Trondheim og Østersund, 1:250.000. *Nor. geol. unders. 353,* 1—76.

Wood, D.A. 1980: The application of a Th-Hf-Ta diagram to problems of tectonomagmatic classification and to establish the nature of crustal contamination of basaltic lavas of the British Tertiary Volcanic Province. *Earth Planet. Sci. Lett. 50,* 11—30.

Wood, D.A., Joron, J.-L. & Treuil, M. 1979: A re-appraisal of the use of trace elements to classify and discriminate between magma series erupted in different tectonic settings. *Earth Planet. Sci. Lett. 45,* 326—336.

Geological map of the Resfjell area, Meldal, western Trondheim region

NGU Bulletin 409 – Heim et al. – Pl. 1

Explanation of legend

(1–11) Resfjell ophiolite fragment

1 – leucogabbro, 2 – microgabbro, 3 – sheeted dyke complex, 4 – dykes or dyke swarms, 5 – transition zone, 6 – lower pillow lavas, 7 – upper pillow lava, 8 – hyaloclastic breccia, 9 – massive lava flows, 10 – jasper horizons, 11 – volcaniclastic sediments

(12–16) Hovin-type sediments, etc.

12 – polymict conglomerate, 13 – silt/sandstone and phyllite, 14 – limestone/marble, 15 – greenstone (undifferentiated), 16 – felsic metavolcanites

The UTM grid is indicated

1 3 5 7 9
2 4 6 8 10 11
12 13 14 15 16

STRIKE & DIP OF:

- Dyke contacts
- Primary bedding: lavas & sediments (inverted, vertical, right way up)
- Paleohorizontal plane: lava shelves
- Thrust fault
- Fault
- Sulphide mineralization
- Prospect

Styrland
Syrstadsætra
Høa
Ljøsåa
Midtfjellet
Rånåsmælbkn.
Storsya
SMÅFJELLA
RESFJELL
GORÅSFJELLET
Snipvatna
VÅLÅSKARET
Mjukinn
Res-vatnet
Ela
Høyløa
Storslåtta
Blautsætra
Otla
Uvøysætra
Vidmyrane
0 1 2km